Spectral scale transformations of nonstationary optical fields

Jyrki Laatikainen,[1,*] Matias Koivurova,[2,3] Jari Turunen,[1] Tero Setälä,[1] and Ari T. Friberg[1]

[1]*Institute of Photonics, University of Eastern Finland, P.O. Box 111, FI-80101 Joensuu, Finland*

[2]*Faculty of Engineering and Natural Sciences, Tampere University, FI-33720 Tampere, Finland*

[3]*Tampere Institute for Advanced Study, Tampere University, FI-33100 Tampere, Finland*

(Received 18 January 2022; accepted 19 July 2022; published 16 August 2022)

The notions of cross-spectral purity and spectral invariance of light impose specific structures for the field coherence. Such concepts were originally introduced for stationary light and recently extended to nonstationary fields. In this work, we establish general conditions for transforming scalar, pulsed, isodiffracting light beams produced, for instance, in usual spherical-mirror laser resonators, to nonstationary secondary sources that exhibit cross-spectral purity or spectral invariance. Further, we introduce hybrid refractive-diffractive imaging systems which perform the desired transformation accurately over a wide spectral range irrespective of the spatial coherence of the incident isodiffracting beam.

DOI: 10.1103/PhysRevA.106.023515

I. INTRODUCTION

Cross-spectral purity [1] and spectral invariance [2] of light are two cornerstone concepts in optical coherence theory. Cross-spectral purity, first proposed by Mandel [1] in 1961, physically amounts to two-beam interference in which the superposition of the two beams exhibits the same normalized spectrum as the input beams do. Spectral invariance, on the other hand, was introduced by Wolf [2] in 1986 and is manifested as light whose spectral properties remain unchanged on free-space propagation; i.e., the far-zone normalized spectrum is directionally invariant and equal to the normalized spectrum across the source. The two phenomena set specific conditions on the form of the coherence function: separability into spatial and temporal parts for cross-spectral purity (the reduction formula) [1,3], and Wolf's scaling law [2] for spectral invariance. The underlying significance of these concepts is that neither purity nor invariance of the spectrum is a general property of light fields, but rather they are features of these special field types. In addition, they enlighten the coherence-induced spectral changes on propagation and interference of light [4–9].

Cross-spectral purity and spectral invariance have been extensively studied for both scalar [10–14] and electromagnetic [15–21] light in stationary conditions but were only recently introduced for nonstationary fields [22–24]. A particularly important class of partially spatially coherent nonstationary fields can be constructed using superpositions of Hermite-Gaussian monochromatic modes of spherical-mirror resonators. These monochromatic modes have the same Rayleigh range for all spatial modes, labeled by index m, and it is also independent of frequency; see, e.g., Sec. 14.7 of Ref. [25]. Hence, each pulsed mode (fixed index m), understood as a spectral superposition of monochromatic modes, has a well-defined Rayleigh range. Likewise, the Rayleigh range of all pulsed fields, obtained by an additional superposition over index m, have the same Rayleigh range. Such fields are called isodiffracting and they satisfy a specific (spectral) isodiffraction condition [26], which differs from the conditions necessitated by cross-spectral purity and spectral invariance.

In this work, we consider the transformation of isodiffracting fields into either cross-spectrally pure or spectrally invariant fields. From previous studies it is known that cross-spectrally pure stationary fields can be generated by an achromatic Fourier transformation [22]. Such an operation can be accomplished by a compensating Fourier-transform system which may be based entirely on refractive lenses or may also contain diffractive elements [27–29]. In the present context, we introduce chromatically compensating imaging (rather than Fourier-transforming) systems which convert isodiffracting fields to either spectrally invariant or cross-spectrally pure fields. We design hybrid (refractive/diffractive) systems that control the spectral magnification so as to realize the desired transformations.

The structure of this paper is as follows. In Sec. II we recall the concepts of cross-spectrally pure, spectrally invariant, and isodiffracting nonstationary light. Then, in Sec. III, we present the physical principles of the required transformations, and in Sec. IV we design afocal first-order imaging systems to realize these transformations with good accuracy. The performance of the transformation systems for broadband light is evaluated in Sec. V. Finally, the main conclusions and some implications of the work are discussed in Sec. VI.

II. CONDITIONS FOR THE FIELD TYPES

Let us consider statistically nonstationary, partially coherent, scalar optical fields in the complex analytic signal representation encompassing only the positive frequencies. In the spectral domain, the field is expressed as $E(\boldsymbol{\rho};\omega)$, where $\boldsymbol{\rho} = (x, y)$ refers to a spatial point and ω is the (angular) frequency. The cross-spectral density (CSD) function between the fields at points $\boldsymbol{\rho}_1$ and $\boldsymbol{\rho}_2$ and frequencies ω_1 and ω_2 is

*Corresponding author: jyrki.laatikainen@uef.fi

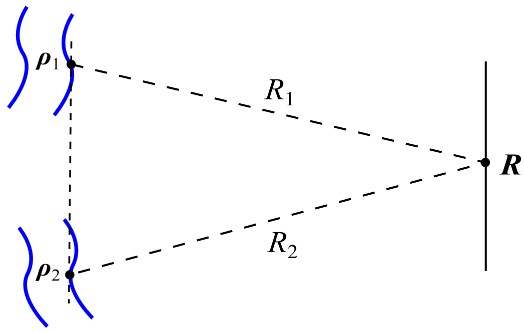

FIG. 1. Superposition of two beams from points $\boldsymbol{\rho}_1$ and $\boldsymbol{\rho}_2$ across a plane, related to the notion of cross-spectral purity.

defined as [30]

$$W(\boldsymbol{\rho}_1, \boldsymbol{\rho}_2; \omega_1, \omega_2) = \langle E^*(\boldsymbol{\rho}_1; \omega_1) E(\boldsymbol{\rho}_2; \omega_2)\rangle, \tag{1}$$

where the angular brackets and the asterisk denote ensemble averaging and complex conjugation, respectively. The spectral density of a nonstationary field is defined as [31–34]

$$S(\boldsymbol{\rho}; \omega) = W(\boldsymbol{\rho}, \boldsymbol{\rho}; \omega, \omega), \tag{2}$$

and its normalized version is expressed as

$$s(\boldsymbol{\rho}; \omega) = \frac{S(\boldsymbol{\rho}; \omega)}{\int_0^\infty S(\boldsymbol{\rho}; \omega) d\omega}. \tag{3}$$

The complex degree of spectral coherence, defined via

$$\mu(\boldsymbol{\rho}_1, \boldsymbol{\rho}_2; \omega_1, \omega_2) = \frac{W(\boldsymbol{\rho}_1, \boldsymbol{\rho}_2; \omega_1, \omega_2)}{[S(\boldsymbol{\rho}_1; \omega_1) S(\boldsymbol{\rho}_2; \omega_2)]^{1/2}}, \tag{4}$$

satisfies the inequalities $0 \leqslant |\mu(\boldsymbol{\rho}_1, \boldsymbol{\rho}_2; \omega_1, \omega_2)| \leqslant 1$, where the lower and upper limits correspond, respectively, to complete incoherence and full coherence of the random field at the values of the arguments.

A. Cross-spectral purity

At some point $\mathbf{R}$, the superposition of the spectral fields emanating from points $\boldsymbol{\rho}_1$ and $\boldsymbol{\rho}_2$ reads as

$$E(\mathbf{R}; \omega) = E(\boldsymbol{\rho}_1; \omega) \exp(i\omega R_1/c) + E(\boldsymbol{\rho}_2; \omega) \exp(i\omega R_2/c), \tag{5}$$

where $R_i = |\boldsymbol{\rho}_i - \mathbf{R}|$, $i \in (1, 2)$, are the distances between the points (see Fig. 1) and c is the vacuum speed of light. The phase difference between the two contributions due to free-space propagation is $\omega\tau = \omega(R_2 - R_1)/c$. The condition for cross-spectral purity is that

$$s(\mathbf{R}; \omega) = s(\boldsymbol{\rho}_1; \omega) = s(\boldsymbol{\rho}_2; \omega) \tag{6}$$

for some value of τ, which thus specifies the point $\mathbf{R}$. The requirements in Eq. (6) are strictly analogous to Mandel's conditions for cross-spectral purity of stationary light [1,3]. In the particular case of $\tau = 0$, purity as given in Eq. (6) is achieved, among other characteristics, if the CSD takes on the form of a product,

$$W(\boldsymbol{\rho}_1, \boldsymbol{\rho}_2; \omega_1, \omega_2) = W_{\rm s}(\boldsymbol{\rho}_1, \boldsymbol{\rho}_2) W_{\rm f}(\omega_1, \omega_2), \tag{7}$$

of planar spatial and spectral factors [22].

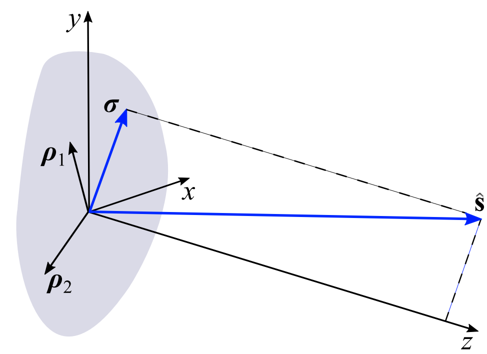

FIG. 2. Notation pertaining to far-field spectral invariance of radiation from a planar secondary source in the xy plane.

B. Spectral invariance

The far-zone spectrum of a nonstationary partially coherent source field characterized by a CSD in Eq. (1) is in the direction specified by the unit vector $\hat{\mathbf{s}}$ (see Fig. 2) given by [23]

$$S^{(\infty)}(\hat{\mathbf{s}}; \omega) = \left(\frac{2\pi s_z}{r}\right)^2 \left(\frac{\omega}{c}\right)^2 T\left(\frac{\omega}{c}\boldsymbol{\sigma}, \frac{\omega}{c}\boldsymbol{\sigma}; \omega, \omega\right). \tag{8}$$

Above,

$$T(\boldsymbol{\kappa}_1, \boldsymbol{\kappa}_2; \omega_1, \omega_2) = \frac{1}{(2\pi)^4} \iint_{-\infty}^{\infty} W(\boldsymbol{\rho}_1, \boldsymbol{\rho}_2; \omega_1, \omega_2) \times \exp[i(\boldsymbol{\kappa}_1 \cdot \boldsymbol{\rho}_1 - \boldsymbol{\kappa}_2 \cdot \boldsymbol{\rho}_2)] d^2\rho_1 d^2\rho_2 \tag{9}$$

is the angular correlation function, $\boldsymbol{\sigma} = (s_x, s_y)$ is the transverse component of $\hat{\mathbf{s}}$, and r is the distance from the source.

A necessary condition for spectral invariance is that the normalized far-field spectrum

$$s^{(\infty)}(\hat{\mathbf{s}}; \omega) = \frac{S^{(\infty)}(\hat{\mathbf{s}}; \omega)}{\int_0^\infty S^{(\infty)}(\hat{\mathbf{s}}; \omega) d\omega} \tag{10}$$

is independent of direction, i.e., $s^{(\infty)}(\hat{\mathbf{s}}; \omega) = s^{(\infty)}(\omega)$. It was established in Ref. [23] that this condition is satisfied if the source-plane CSD is of the form

$$W(\boldsymbol{\rho}_1, \boldsymbol{\rho}_2; \omega_1, \omega_2) = [S(\bar{\boldsymbol{\rho}}; \omega_1) S(\bar{\boldsymbol{\rho}}; \omega_2)]^{1/2} \times g(\boldsymbol{\rho}_1, \boldsymbol{\rho}_2; \omega_1, \omega_2), \tag{11}$$

where $g(\boldsymbol{\rho}_1, \boldsymbol{\rho}_2; \omega_1, \omega_2)$ obeys the boundary condition

$$g(\boldsymbol{\rho}_1, \boldsymbol{\rho}_2; \omega, \omega) = \nu(\Delta\boldsymbol{\rho}; \omega) = \frac{H(\omega\Delta\boldsymbol{\rho}/c)}{H(0)}, \tag{12}$$

and $\bar{\boldsymbol{\rho}} = (\boldsymbol{\rho}_1 + \boldsymbol{\rho}_2)/2$ and $\Delta\boldsymbol{\rho} = \boldsymbol{\rho}_2 - \boldsymbol{\rho}_1$ denote the average and difference source-plane spatial coordinates. It then follows that $s^{(\infty)}(\omega)$ is equal to the normalized form

$$\bar{s}(\omega) = \frac{S^{(\rm int)}(\omega)}{\int_0^\infty S^{(\rm int)}(\omega) d\omega} \tag{13}$$

of the source-integrated spectral density

$$S^{(\rm int)}(\omega) = \int_{-\infty}^{\infty} S(\boldsymbol{\rho}; \omega) d^2\rho, \tag{14}$$

i.e., we have the equality $s^{(\infty)}(\omega) = \bar{s}(\omega)$.

The scaling law for nonstationary fields, expressed by Eqs. (11) and (12), reduces to Wolf's original scaling law [2] for stationary and quasihomogeous fields.

C. Isodiffracting fields

The CSD of any stationary field can be represented as an incoherent superposition of fully coherent modal fields [30], and a corresponding representation is available also for nonstationary fields [35,36]. If the modal fields are separable in Cartesian coordinates as

$$\psi_{mn}(x, y; \omega) = \psi_m(x; \omega)\psi_n(y; \omega), \tag{15}$$

where m and n are nonnegative integers, also the CSD is of the separable form

$$W(\boldsymbol{\rho}_1, \boldsymbol{\rho}_2; \omega_1, \omega_2) = W(x_1, x_2; \omega_1, \omega_2)W(y_1, y_2; \omega_1, \omega_2), \tag{16}$$

where

$$W(x_1, x_2; \omega_1, \omega_2) = \sum_{m=0}^{\infty} c_m \psi_m^*(x_1; \omega_1)\psi_m(x_2; \omega_2) \tag{17}$$

and an analogous expression applies to $W(y_1, y_2; \omega_1, \omega_2)$. Here the coefficients c_m are nonnegative and frequency independent.

Let us, in particular, consider Hermite-Gaussian modal fields of the form

$$\psi_m(x; \omega) = [S_0(\omega)]^{1/4} \frac{(2/\pi)^{1/4}}{\sqrt{2^m m! w_0(\omega)}} \times H_m\left[\frac{\sqrt{2}x}{w_0(\omega)}\right] \exp\left[-\frac{x^2}{w_0^2(\omega)}\right], \tag{18}$$

where H_m is a Hermite polynomial of order m, $w_0(\omega)$ is the frequency-dependent spatial beam width at the waist, and $S_0(\omega)$ is the spectral weight function of the mode. Pulsed modes of this type are generated in the usual paraxial spherical-mirror cavities. The Rayleigh range $z_R = \pi w_0^2(\omega)/\lambda$, where λ is the wavelength, is frequency independent for each spatial mode produced in such a cavity [25]. Therefore, the beam width $w_0(\omega)$ must follow the condition

$$w_0(\omega) = \sqrt{\frac{\omega_0}{\omega}} w_0, \tag{19}$$

where $w_0 = w_0(\omega_0)$ and ω_0 is a reference frequency such as the mean frequency of $S_0(\omega)$. The pulsed beams emerging from the cavity then expand upon propagation at the same rate at each frequency ω, thus being sometimes called isodiffracting [26]. Therefore, we refer to Eq. (19) as the isodiffraction condition.

Since the requirement in Eq. (19) applies to each individual mode, the property of isodiffraction is shared by all superpositions of the form of Eq. (17), regardless of the distribution of the coefficients c_m. A particularly important case, however, is

$$c_m = w_0 \sqrt{\frac{2\pi}{\beta}} \frac{1}{1 + 1/\beta} \left(\frac{1 - \beta}{1 + \beta}\right)^m, \tag{20}$$

where the parameter β is bounded as $0 \leqslant \beta \leqslant 1$. This leads to pulsed isodiffracting partially coherent beams that are spatially of the Gaussian Schell-model (GSM) type [26]. With this choice of the coefficients the CSD assumes a compact analytical form:

$$W(\boldsymbol{\rho}_1, \boldsymbol{\rho}_2; \omega_1, \omega_2) = \left(\frac{\omega_1}{\omega_0}\frac{\omega_2}{\omega_0}\right)^{1/2} [S_0(\omega_1)S_0(\omega_2)]^{1/2} \times \exp\left(-\frac{1 + \beta^2}{2\beta} \frac{\omega_1 \boldsymbol{\rho}_1^2 + \omega_2 \boldsymbol{\rho}_2^2}{\omega_0 w_0^2}\right) \times \exp\left(\frac{1 - \beta^2}{\beta} \frac{\sqrt{\omega_1\omega_2}}{\omega_0} \frac{\boldsymbol{\rho}_1 \cdot \boldsymbol{\rho}_2}{w_0^2}\right). \tag{21}$$

The field is spatially fully coherent when $\beta = 1$, is spatially quasihomogeneous when $\beta \ll 1$, and becomes spatially incoherent when $\beta \to 0$. The GSM fields have convenient mathematical properties and in the present context allow one to assess analytically the transformations of partially coherent isodiffracting fields. Consequently, they provide significant physical insight into the performed operations and, therefore, we adopt the GSM pulsed beams in the analysis to follow.

III. TRANSFORMATION SYSTEMS

We proceed to examine the possibilities to transform isodiffracting fields to either cross-spectrally pure or spectrally invariant fields using paraxial optical systems described by *ABCD* matrices. In particular, we consider an afocal imaging system whose frequency-dependent system matrix is given by [37]

$$\mathbf{M}(\omega) = \begin{bmatrix} A(\omega) & B(\omega) \\ C(\omega) & D(\omega) \end{bmatrix} = \begin{bmatrix} M(\omega) & 0 \\ 0 & 1/M(\omega) \end{bmatrix}, \tag{22}$$

where $M(\omega)$ is the (spectral) magnification of the system. If we denote the field at the input plane of the system by $E_0(\boldsymbol{\rho}; \omega)$, the field at the output plane is

$$E(\boldsymbol{\rho}; \omega) = \frac{\exp(i\omega L/c)}{M(\omega)} E_0\left[\frac{\boldsymbol{\rho}}{M(\omega)}; \omega\right], \tag{23}$$

where L is the axial path length from the input plane to the output plane. This result can be formally established by considering the traditional lens-system diffraction formula [38] and using the method of a stationary phase (see Ref. [30], Sec. 3.3.3) in the asymptotic limit $B(\omega) \to 0$ in Eq. (22).

Inserting Eq. (23) into Eq. (1) gives a relation between the output-plane CSD and the input-plane $W_0(\boldsymbol{\rho}_1, \boldsymbol{\rho}_2; \omega_1, \omega_2)$ in the form

$$W(\boldsymbol{\rho}_1, \boldsymbol{\rho}_2; \omega_1, \omega_2) = \frac{\exp(i\Delta\omega L/c)}{M(\omega_1)M(\omega_2)} \times W_0\left[\frac{\boldsymbol{\rho}_1}{M(\omega_1)}, \frac{\boldsymbol{\rho}_2}{M(\omega_2)}; \omega_1, \omega_2\right], \tag{24}$$

where $\Delta\omega = \omega_2 - \omega_1$. Considering a CSD of the form of Eq. (21) at the input plane and carrying out a derivation analogous to that in Ref. [23] gives the result

$$W(\boldsymbol{\rho}_1, \boldsymbol{\rho}_2; \omega_1, \omega_2) = \frac{\exp(i\Delta\omega L/c)}{M(\omega_1)M(\omega_2)}\left(\frac{\omega_1}{\omega_0}\frac{\omega_2}{\omega_0}\right)^{1/2}[S_0(\omega_1)S_0(\omega_2)]^{1/2} \times \exp\left\{-\frac{1+\beta^2}{2\beta}\left[\frac{\omega_1}{\omega_0}\frac{\boldsymbol{\rho}_1^2}{M^2(\omega_1)w_0^2} + \frac{\omega_2}{\omega_0}\frac{\boldsymbol{\rho}_2^2}{M^2(\omega_2)w_0^2}\right]\right\} \times \exp\left[\frac{1-\beta^2}{\beta}\frac{\sqrt{\omega_1\omega_2}}{\omega_0}\frac{\boldsymbol{\rho}_1\cdot\boldsymbol{\rho}_2}{M(\omega_1)M(\omega_2)w_0^2}\right] \quad (25)$$

at the output plane. The related spectral density takes the form

$$S(\boldsymbol{\rho}, \omega) = \frac{S_0(\omega)}{M^2(\omega)}\frac{\omega}{\omega_0}\exp\left[-\frac{\omega}{\omega_0}\frac{2\boldsymbol{\rho}^2}{M^2(\omega)w^2}\right], \quad (26)$$

where we have denoted by

$$w = w_0/\sqrt{\beta} \quad (27)$$

the $1/e^2$ width of the output spatial intensity profile at $\omega = \omega_0$ and unit magnification. This is wider, by a coherence-dependent factor of $1/\sqrt{\beta}$, than the width of the fundamental Gaussian mode $m = n = 0$ in the coherent-mode expansion of the CSD.

A. Cross-spectral purity

For producing a cross-spectrally pure beam field we investigate systems with spectral magnification of the form

$$M(\omega) = \sqrt{\frac{\omega}{\omega_0}}\, M_0, \quad (28)$$

where $M_0 = M(\omega_0)$. For a GSM input field, Eq. (25) gives an output-plane CSD in the form of Eq. (7), with

$$W_s(\boldsymbol{\rho}_1, \boldsymbol{\rho}_2) = \frac{1}{M_0^2}\exp\left(-\frac{1+\beta^2}{2\beta^2}\frac{\boldsymbol{\rho}_1^2+\boldsymbol{\rho}_2^2}{M_0^2w^2}\right) \times \exp\left(\frac{1-\beta^2}{\beta^2}\frac{\boldsymbol{\rho}_1\cdot\boldsymbol{\rho}_2}{M_0^2w^2}\right) \quad (29)$$

and

$$W_f(\omega_1, \omega_2) = \exp(i\Delta\omega L/c)[S_0(\omega_1)S_0(\omega_2)]^{1/2}, \quad (30)$$

where we have used Eq. (27). Hence, the CSD factors into two functions containing spatial and spectral contributions separately, as in Eq. (7), which ensures that the output field is cross-spectrally pure.

In addition, evaluating Eqs. (29) and (30) at a single spatiospectral point and employing Eq. (3), we find the normalized spectral density

$$s(\boldsymbol{\rho}; \omega) = \frac{S_0(\omega)}{\int_0^\infty S_0(\omega)d\omega}, \quad (31)$$

which is independent of the spatial position conforming to the latter equality in Eq. (6). It should be noted, however, that the above conclusions apply only to the field at the output plane of the system. Cross-spectral purity is not preserved upon propagation because of the frequency dependence of the diffraction phenomena, which introduces space-frequency coupling.

B. Spectral invariance

In order to satisfy the scaling-law conditions in Eqs. (11) and (12), we examine a system whose spectral magnification is of the form

$$M(\omega) = \sqrt{\frac{\omega_0}{\omega}}\, M_0. \quad (32)$$

Considering again a GSM input field, we arrive at the result

$$W(\boldsymbol{\rho}_1, \boldsymbol{\rho}_2; \omega_1, \omega_2) = \frac{\exp(i\Delta\omega L/c)}{M_0^2}\frac{\omega_1}{\omega_0}\frac{\omega_2}{\omega_0}[S_0(\omega_1)S_0(\omega_2)]^{1/2} \times \exp\left(-\frac{1+\beta^2}{2\beta}\frac{\omega_1^2\boldsymbol{\rho}_1^2+\omega_2^2\boldsymbol{\rho}_2^2}{\omega_0^2M_0^2w_0^2}\right) \times \exp\left[\frac{1-\beta^2}{\beta}\left(\frac{\omega_1}{\omega_0}\frac{\omega_2}{\omega_0}\right)\frac{\boldsymbol{\rho}_1\cdot\boldsymbol{\rho}_2}{M_0^2w_0^2}\right]. \quad (33)$$

The spectral density and the complex degree of spectral coherence take the forms

$$S(\boldsymbol{\rho}; \omega) = \frac{S_0(\omega)}{M_0^2}\left(\frac{\omega}{\omega_0}\right)^2\exp\left[-\left(\frac{\omega}{\omega_0}\right)^2\frac{2\boldsymbol{\rho}^2}{M_0^2w^2}\right] \quad (34)$$

and

$$\mu(\boldsymbol{\rho}_1, \boldsymbol{\rho}_2; \omega_1, \omega_2) = \exp(i\Delta\omega L/c) \times \exp\left[-\frac{1-\beta^2}{2\beta^2}\frac{(\omega_1\boldsymbol{\rho}_1-\omega_2\boldsymbol{\rho}_2)^2}{\omega_0^2M_0^2w^2}\right], \quad (35)$$

respectively, where Eq. (27) is again used. This result shows that the complex degree of spectral coherence at any single point $\boldsymbol{\rho}_1 = \boldsymbol{\rho}_2 = \boldsymbol{\rho} > 0$ is partial, i.e., $|\mu(\boldsymbol{\rho}, \boldsymbol{\rho}; \omega_1, \omega_2)| < 1$, unless $\beta = 1$. In other words, partial spatial coherence generally implies partial spectral coherence because of space-frequency coupling.

To establish that the CSD in Eq. (33) is of the spectrally invariant form we express it in terms of average and difference spatial coordinates and additionally employ the corresponding spectral coordinates $\bar{\omega} = (\omega_1+\omega_2)/2$ and $\Delta\omega$. This yields a result in the form of Eq. (11) with $S(\bar{\boldsymbol{\rho}}; \omega)$ having the form of Eq. (34) and

$$g(\bar{\boldsymbol{\rho}}, \Delta\boldsymbol{\rho}; \bar{\omega}, \Delta\omega) = \exp(i\Delta\omega L/c) \times \exp\left[-\left(\frac{\Delta\omega}{\omega_0}\right)^2\left(\frac{1}{\beta^2}-1\right)\frac{\bar{\boldsymbol{\rho}}^2}{2M_0^2w^2}\right] \times \exp\left[-\left(\frac{\bar{\omega}}{\omega_0}\right)^2\frac{\Delta\boldsymbol{\rho}^2}{2M_0^2w^2\beta^2}\right] \times \exp\left(-\frac{\bar{\omega}\Delta\omega}{\omega_0^2}\frac{1+\beta^2}{\beta^2}\frac{\bar{\boldsymbol{\rho}}\Delta\boldsymbol{\rho}}{M_0^2w^2}\right) \times \exp\left[-\left(\frac{\Delta\omega}{\omega_0}\right)^2\frac{\Delta\boldsymbol{\rho}^2}{8M_0^2w^2}\right]. \quad (36)$$

We therefore have

$$\nu(\Delta\boldsymbol{\rho}; \omega) = \exp\left[-\left(\frac{\omega}{\omega_0}\right)^2\frac{\Delta\boldsymbol{\rho}^2}{2M_0^2w^2\beta^2}\right], \quad (37)$$

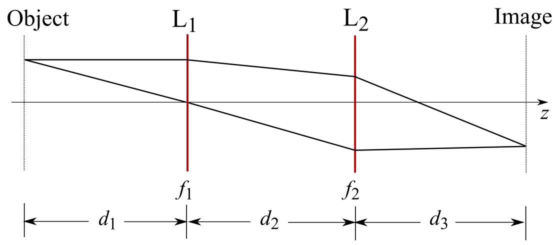

FIG. 3. Lens system geometry: L_1 and L_2 are (refractive or diffractive) thin lenses with focal lengths f_1 and f_2. The object (input) plane, the lenses, and the image (output) plane are separated by distances d_1, d_2, and d_3 that, along with f_1 and f_2, constitute the set of design parameters.

which satisfies the condition (12) for spectrally invariant nonstationary fields.

The normalized source-integrated spectrum, obtained by inserting from Eq. (34) into Eq. (13), is simply the normalized form of $S_0(\omega)$, i.e.,

$$\bar{s}(\omega) = \frac{S_0(\omega)}{\int_0^\infty S_0(\omega)d\omega} = s^{(\infty)}(\omega). \tag{38}$$

The latter equality follows directly from the scaling law and can be verified by inserting the CSD in Eq. (33) into Eq. (9) and using Eqs. (8) and (10).

IV. OPTICAL SYSTEM DESIGN

We have so far established that ideal afocal imaging systems can transform isodiffracting input beams into a cross-spectrally pure form if the spectral magnification follows Eq. (28), or into a spectrally invariant form if the magnification is as specified in Eq. (32). Next we describe how such transformations can be achieved in practice with high accuracy.

First-order systems based on purely refractive lenses are known to enable an achromatic Fourier transform [27,28]. However, the addition of highly dispersive diffractive lenses adds a new degree of freedom in the design of such spectrally compensating systems [29]. Expecting the same to be true for imaging (rather than Fourier-transforming) systems, we therefore consider hybrid afocal systems consisting of one (ideal achromatic) refractive lens of focal length f_r and one diffractive lens with a frequency-dependent focal length [39]

$$f_\mathrm{d}(\omega) = \frac{\omega}{\omega_0} f_\mathrm{d}, \tag{39}$$

where $f_\mathrm{d} = f_\mathrm{d}(\omega_0)$. The above expression shows that the focal length of the diffractive element has a linear frequency dependence, which is characteristic of all diffractive lenses. The configuration of the two-lens system is shown in Fig. 3. The designs to be presented below are based on the thin-element approximation. However, neither the residual chromatic aberration nor the finite lens-element thicknesses of real achromats, or the finite substrate thickness of the diffractive lens, have a significant effect on system performance as long as the principal planes of L_1 and L_2 are set at the designed positions.

A. Cross-spectral purity

For cross-spectrally pure output, the achromat is positioned before the diffractive lens, i.e., $f_1 = f_\mathrm{r}$ and $f_2 = f_\mathrm{d}$ in Fig. 3. After implementing the condition presented in Eq. (28) for system magnification, together with the requirements in Eq. (22) for an afocal imaging system at the reference wavelength, we arrive at the conditions

$$d_1 = f_\mathrm{r} + \frac{f_\mathrm{r}^2}{2f_\mathrm{d}}, \tag{40a}$$

$$d_2 = f_\mathrm{d} + f_\mathrm{r}, \tag{40b}$$

$$d_3 = \frac{f_\mathrm{d}}{2} \tag{40c}$$

for the lens separations. These distances are positive as long as both f_r and $f_\mathrm{d}(\omega_0)$ are selected to be positive. The system matrix elements of a thin-lens setup which fulfils the conditions given above will be exactly of the form presented in Eq. (28) when $\omega = \omega_0$. Hence, an afocal imaging system is achieved at the reference wavelength. The performance at other frequencies is obtained by calculating the *ABCD* ray-transfer matrix for the setup in Fig. 3 with $f_1 = f_\mathrm{r}$ and $f_2 = f_\mathrm{d}(\omega)$ as in Eq. (39) and the lens separations given in Eqs. (40a)–(40c). Using Eq. (22), we find that the magnification is

$$M(\omega) = \frac{3\omega - \omega_0}{2\omega} M_0, \tag{41}$$

which at ω_0 coincides with the exact magnification given in Eq. (28) and approximates that at other frequencies. The accuracy of the approximation is illustrated in Fig. 4(a). We see that the condition of cross-spectral purity is satisfied with high precision for a relatively wide spectral range around ω_0.

B. Spectral invariance

When a spectrally invariant output field is pursued, the arrangement of the two lenses is reversed with $f_1 = f_\mathrm{d}$ and $f_2 = f_\mathrm{r}$ in the geometry of Fig. 3. By following a similar procedure as previously, the expressions

$$d_1 = \frac{f_\mathrm{d}}{2}, \tag{42a}$$

$$d_2 = f_\mathrm{d} + f_\mathrm{r}, \tag{42b}$$

$$d_3 = f_\mathrm{r} + \frac{f_\mathrm{r}^2}{2f_\mathrm{d}} \tag{42c}$$

are obtained for the system distances. The system matrix will then again satisfy the conditions of Eq. (22), with magnification

$$M(\omega) = \frac{\omega + \omega_0}{2\omega} M_0. \tag{43}$$

Figure 4(b) shows the accuracy at which this expression approximates the ideal condition of Eq. (32). We observe from the figure that the approximate magnification in the case of spectral invariance remains highly accurate over a wider range compared with the analogous result for cross-spectral purity.

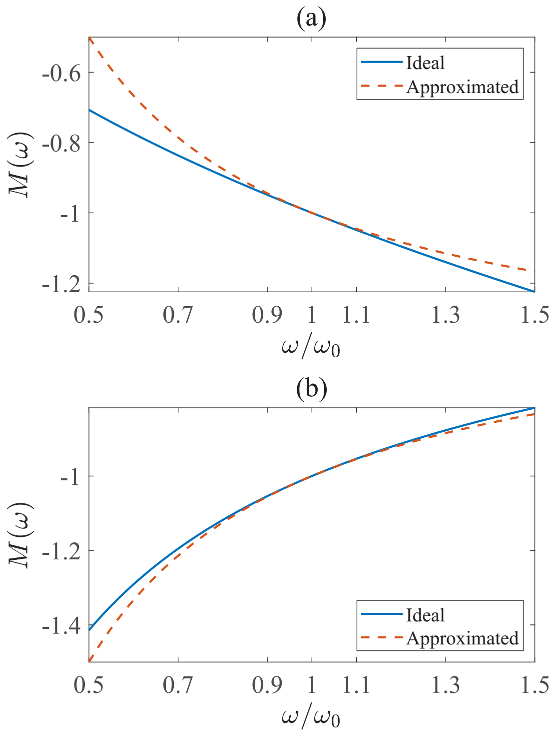

FIG. 4. Comparison between the ideal and approximated conditions for (a) cross-spectral purity and (b) spectral invariance at output in terms of the magnification $M(\omega)$ of the transformation system (for $M_0 = -1$).

V. SYSTEM PERFORMANCE FOR BROADBAND LIGHT

It is clear from Fig. 4 that the approximative magnifications are excellent around the reference frequency ω_0 but the deviations from the ideal cases grow with the increase of the spectral width of the field. To investigate how this affects the transformation of isodiffracting input to either cross-spectrally pure or spectrally invariant output, we consider a model spectrum $S_0(\omega)$ of the power-exponential form [26,40,41]

$$[S_0(\omega)]^{1/4} = \left(\frac{\omega_0}{\omega}\right)^{1/4} \frac{1}{\sqrt{\Gamma(2p)}} \left(2p\frac{\omega}{\omega_0}\right)^p \exp\left(-p\frac{\omega}{\omega_0}\right), \tag{44}$$

where p is a real positive constant that can be varied to control the spectral bandwidth of the pulse train, ω_0 is the mean frequency, and $\Gamma(x)$ is the gamma function. As discussed more extensively in Ref. [26], the choice of p connects the weight function to different regimes of optical pulses. In general, the pulses are in the subcycle regime when $p < 10$, in the single-cycle regime when $p \sim 15$, and in the few-cycle regime when $p \sim 50$. This spectrum, though asymmetric, is mathematically convenient since it contains no negative frequencies but yet approaches a Gaussian spectrum when p increases, in which case the mean frequency ω_0 becomes the peak frequency.

A. Cross-spectral purity

For the output field to be cross-spectrally pure, its normalized spectrum at every spatial point should be as in Eq. (31). If,

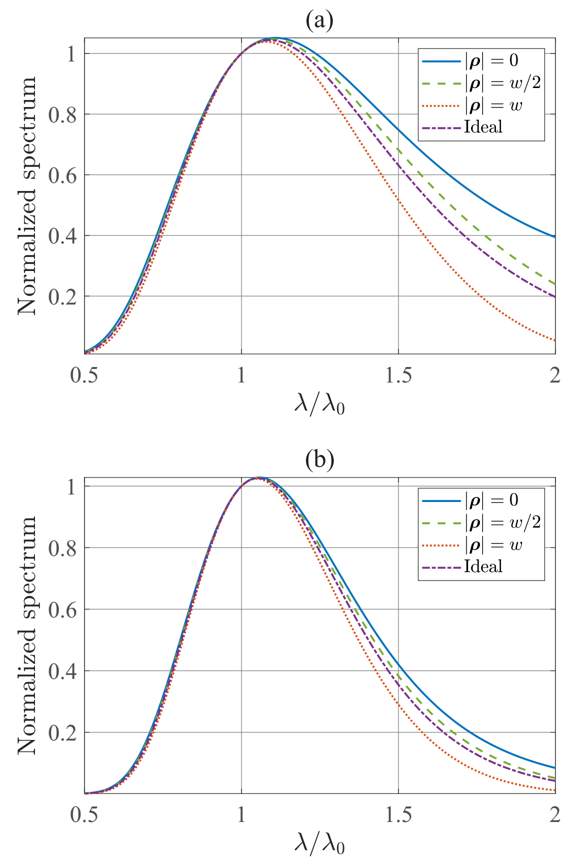

FIG. 5. Normalized spectra of an ideal cross-spectrally pure field and the spectra obtained by the approximative system magnification at three spatial points when (a) $p = 3$ and (b) $p = 5$. The spectra are plotted with respect to λ/λ_0 and normalized to their values at $\lambda = \lambda_0$ for clarity.

however, we insert the magnification in Eq. (41) into Eq. (26), we see that this is not strictly true even at the on-axis point $\boldsymbol{\rho} = 0$.

Figure 5 shows the ideal normalized spectrum given by Eq. (31) along with the normalized spectra obtained with the approximate $M(\omega)$ at three radial positions: $|\boldsymbol{\rho}| = 0$, $|\boldsymbol{\rho}| = w/2$, and $|\boldsymbol{\rho}| = w$. The normalization in Eq. (3) was accomplished with numerical integration using Eq. (A1) in the Appendix, and the results are plotted for $p = 3$ and $p = 5$. In addition, the curves are further normalized to their values at $\lambda = \lambda_0$. Note that due to asymmetry, the model spectrum in Eq. (44) does not assume its maximum value at λ_0 and, consequently, the normalized spectra take on values larger than unity. The approximation produces nearly cross-spectrally pure output fields, apart from the long-wavelength region, already at $p \sim 5$, and the curves become nearly indistinguishable (not shown) if $p > 10$. Here we have plotted the results only up to $\lambda = 2\lambda_0$ ($\lambda_0 = 2\pi c/\omega_0$), since if we choose the center wavelength in the middle of the visible spectrum ($\lambda_0 = 550$ nm), $2\lambda_0$ corresponds to the band-gap wavelength of a silicon photodetector. We see, in particular, that the approximated spectrum is wider than the ideal at points close to the optical axis, but narrower well outside the axis.

B. Spectral invariance

An ideal spectrally invariant output field should satisfy the equalities in Eq. (38), but again the approximative spectral magnification in Eq. (43) causes deviations from the ideal performance. The source-integrated spectral density is obtained by inserting from Eq. (26) into Eq. (14), and the result is $S^{(\text{int})}(\omega) = S_0(\omega)\pi w^2/2$ irrespective of the spectral magnification. Hence the first equality in Eq. (38) always holds, but the second one does not.

For the far-field analysis we insert the CSD in Eq. (25) into Eq. (9) and set $\omega_1 = \omega_2$, which yields

$$T\left(\frac{\omega}{c}\boldsymbol{\sigma};\frac{\omega}{c}\boldsymbol{\sigma};\omega,\omega\right) = \frac{1}{(2\pi)^4}\frac{\omega}{\omega_0}\frac{S_0(\omega)}{M^2(\omega)}\iint_{-\infty}^{\infty}\exp\left[-\frac{1+\beta^2}{2\beta}\frac{\omega}{\omega_0}\frac{\boldsymbol{\rho}_1^2+\boldsymbol{\rho}_2^2}{M^2(\omega)w_0^2}\right] \times \exp\left[\frac{1-\beta^2}{\beta}\frac{\omega}{\omega_0}\frac{\boldsymbol{\rho}_1\cdot\boldsymbol{\rho}_2}{M^2(\omega)w_0^2}\right] \times \exp\left[i(\omega/c)(\boldsymbol{\sigma}\cdot\boldsymbol{\rho}_1 - \boldsymbol{\sigma}\cdot\boldsymbol{\rho}_2)\right]d^2\rho_1 d^2\rho_2. \tag{45}$$

The integrals in this expression can be evaluated with Eq. (A2). This leads to

$$T\left(\frac{\omega}{c}\boldsymbol{\sigma};\frac{\omega}{c}\boldsymbol{\sigma};\omega,\omega\right) = \frac{1}{16\pi^2}\frac{\omega_0}{\omega}S_0(\omega)M^2(\omega)w^4\beta^2 \times \exp\left[-\frac{k_0^2}{2}\frac{\omega}{\omega_0}M^2(\omega)w^2\beta^2|\boldsymbol{\sigma}|^2\right], \tag{46}$$

where $k_0 = \omega_0/c$. The far-field spectrum is obtained by inserting the above expression into Eq. (8), with the result

$$S^{(\infty)}(\theta;\omega) = \frac{k_0^2}{4r^2}\frac{\omega}{\omega_0}S_0(\omega)M^2(\omega)w^4\beta^2\cos^2\theta \times \exp\left[-\frac{k_0^2}{2}\frac{\omega}{\omega_0}M^2(\omega)w^2\beta^2\sin^2\theta\right], \tag{47}$$

where the angle θ satisfies $s_z = \cos\theta$ and $|\boldsymbol{\sigma}| = \sin\theta$. In the ideal case of Eq. (32) the far-field spectrum can be written in the form

$$S^{(\infty)}(\theta;\omega) = S_0(\omega)\left(\frac{w\cos\theta}{r\sin\vartheta}\right)^2\exp\left(-2\frac{\sin^2\theta}{\sin^2\vartheta}\right), \tag{48}$$

where we have introduced an $1/e^2$ divergence angle ϑ by

$$\sin\vartheta = \frac{\lambda_0}{\pi M_0 w\beta}. \tag{49}$$

Hence the normalized spectrum is directionally invariant as seen by recalling Eq. (10). Moreover, all partially coherent fields with the same value of the product $w\beta$ are equivalent regarding their far-zone radiation patterns. This feature is analogous to the equivalence theorem for radiation patterns of stationary GSM fields [30].

Figure 6 illustrates the spatially averaged source spectrum and the far-zone normalized spectra if the approximation of the magnification is made according to Eq. (43). The normalization is again accomplished with Eq. (A1), and we consider the cases of $p = 3$ and $p = 5$ at three different angles: $\theta = 0$, $\theta = \vartheta/2$, and $\theta = \vartheta$. Furthermore, the spectra are again scaled to their values at $\lambda = \lambda_0$. Since the approximation is more accurate for the spectral-invariance transformation than for the purity transformation, the results are even closer to the ideal case also in the long-wavelength regime. We see that the axial spectral width is slightly larger than the width of the source-averaged spectrum, but it narrows to some degree when the angle θ increases.

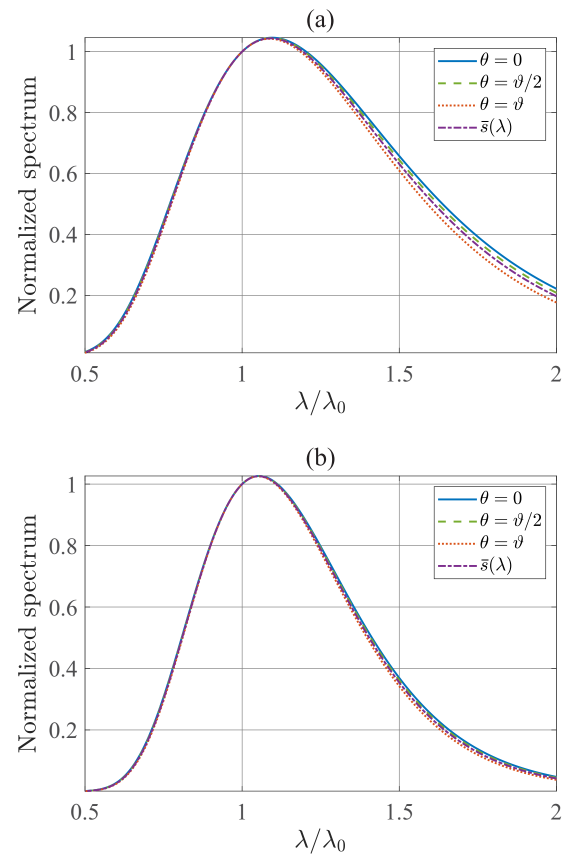

FIG. 6. Normalized far-field spectra together with the normalized source-averaged spectrum in the case of the approximate spectral magnification given in Eq. (43), for angles $\theta = 0$, $\theta = \vartheta/2$, and $\theta = \vartheta$ when (a) $p = 3$ and (b) $p = 5$. The spectra are normalized to their values at $\lambda_0 = w/6$.

To experimentally verify the results presented above, one would be interested in the spatial dependence of the ensemble-averaged spectrum of the nonstationary field. Specifically, one would measure the time-integrated form of the time-dependent physical spectrum [42] of the pulsed field. The results of such measurements are instrument-dependent and provide a smoothed version of the spectrum in Eq. (2) as discussed in Ref. [43].

VI. CONCLUSIONS

In this work, we studied the transformation of nonstationary (pulsed) isodiffracting fields into either cross-spectrally pure or spectrally invariant fields. For this purpose we introduced the conditions for an afocal *ABCD* imaging system to realize the pursued transformations exactly. In addition, for implementing the transformations we presented first-order optical systems that are hybrid lens designs consisting of an achromatic and a diffractive lens. While the spectral magnification of such systems is only an approximation of the ideal, we showed that the desired transformations can be accomplished at high precision even for broadband light.

ACKNOWLEDGMENTS

This work was supported by the Academy of Finland via Projects No. 333938 and No. 308393 and the Flagship Programme, Photonics Research and Innovation (PREIN, Grants No. 320165 and No. 320166).

APPENDIX

The trapezoidal rule used to normalize the spectra in Figs. 5 and 6 reads as

$$\int_a^b f(x)dx \approx \frac{b-a}{2N}\sum_{n=1}^{N}[f(x_n)+f(x_{n+1})], \tag{A1}$$

where N is the number of points inside an equispaced division of the interval (a, b) (see p. 253 of Ref. [44]). We also need the integral formula

$$\int_{-\infty}^{\infty} \exp\left(-ax^2 \pm bx\right)dx = \sqrt{\frac{\pi}{a}}\exp\left(\frac{b^2}{4a}\right), \quad \mathrm{Re}\,a > 0, \tag{A2}$$

which can be found from Ref. [45], p. 337.

[1] L. Mandel, Concept of cross-spectral purity in coherence theory, J. Opt. Soc. Am. **51**, 1342 (1961).

[2] E. Wolf, Invariance of the Spectrum of Light on Propagation, Phys. Rev. Lett. **56**, 1370 (1986).

[3] L. Mandel and E. Wolf, Spectral coherence and the concept of cross-spectral purity, J. Opt. Soc. Am. **66**, 529 (1976).

[4] E. Wolf, Non-cosmological redshifts of spectral lines, Nature (London) **326**, 363 (1987).

[5] E. Wolf, Red Shifts and Blue Shifts of Spectral Lines Emitted by Two Correlated Sources, Phys. Rev. Lett. **58**, 2646 (1987).

[6] M. F. Bocko, D. H. Douglas, and R. S. Know, Observation of Frequency Shifts of Spectral Lines Due to Source Correlations, Phys. Rev. Lett. **58**, 2649 (1987).

[7] G. M. Morris and D. Faklis, Effects of source correlation on the spectra of light, Opt. Commun. **62**, 5 (1987).

[8] F. Gori, G. Guattari, C. Palma, and C. Padovani, Observation of optical redshifts and blueshifts produced by source correlations, Opt. Commun. **67**, 1 (1988).

[9] E. Wolf and D. F. V. James, Correlation-induced spectral changes, Rep. Prog. Phys. **59**, 771 (1996).

[10] F. Gori, G. L. Marcopoli, and M. Santarsiero, Spectrum invariance on paraxial propagation, Opt. Commun. **81**, 123 (1991).

[11] D. F. V. James and E. Wolf, Cross-spectrally pure light and the spectral modulation law, Opt. Commun. **138**, 257 (1997).

[12] H. Roychowdhury and E. Wolf, Spectral invariance in fields generated by quasi-homogeneous scaling law sources, Opt. Commun. **215**, 199 (2003).

[13] H. Liu, J. Cheng, and S. Han, Cross-spectral purity and its influence in ghost imaging experiments, Opt. Commun. **273**, 50 (2007).

[14] M. Lahiri and E. Wolf, Statistical similarity and cross-spectral purity of stationary stochastic fields, Opt. Lett. **37**, 963 (2012).

[15] J. X. Pu, O. Korotkova, and E. Wolf, Polarization-induced spectral changes on propagation of stochastic electromagnetic beams, Phys. Rev. E **75**, 056610 (2007).

[16] T. Hassinen, J. Tervo, and A. T. Friberg, Cross-spectral purity of electromagnetic fields, Opt. Lett. **34**, 3866 (2009).

[17] T. Hassinen, J. Tervo, T. Setälä, J. Turunen, and A. T. Friberg, Spectral invariance and the scaling law with random electromagnetic fields, Phys. Rev. A **88**, 043804 (2013).

[18] T. Hassinen, J. Tervo, and A. T. Friberg, Cross-spectral purity of the Stokes parameters, Appl. Phys. B **105**, 305 (2011).

[19] T. Hassinen, J. Tervo, and A. T. Friberg, Purity of partial polarization in the frequency and time domains, Opt. Lett. **38**, 1221 (2013).

[20] J. Chen, R. Lu, F. Chen, and J. Li, Cross-spectrally pure light, cross-spectrally pure fields and statistical similarity in electromagnetic fields, J. Mod. Opt. **61**, 1164 (2014).

[21] X. Peng, D. Ye, Y. Xin, Y. Chen, and M. Song, Cross-spectral purity of Stokes parameters, purity of partial polarization and statistical similarity, Optik **145**, 42 (2017).

[22] M. Koivurova, C. Ding, J. Turunen, and A. T. Friberg, Cross-spectral purity of nonstationary light, Phys. Rev. A **99**, 043842 (2019).

[23] C. Ding, M. Koivurova, T. Setälä, J. Turunen, and A. T. Friberg, Spectral invariance and scaling law for nonstationary optical fields, Phys. Rev. A **101**, 033808 (2020).

[24] R. Joshi and B. Kanseri, Cross-spectral purity of nonstationary vector fields in space-time and space-frequency domains, J. Opt. Soc. Am. A **38**, 271 (2021).

[25] P. W. Milonni and J. H. Eberly, *Lasers* (Wiley, New York, 1988).

[26] M. Koivurova, C. Ding, J. Turunen, and L. Pan, Partially coherent isodiffracting pulsed beams, Phys. Rev. A **97**, 023825 (2018).

[27] R. H. Katyl, Compensating optical systems. Part 3: Achromatic Fourier transformation, Appl. Opt. **11**, 1255 (1972).

[28] G. M. Morris, An ideal achromatic Fourier processer, Opt. Commun. **39**, 143 (1981).

[29] E. Tajahuerce, V. Climent, J. Lancis, M. Fernandez-Alonso, and P. Andres, Achromatic Fourier transforming properties of a separated diffractive lens doublet: theory and experiment, Appl. Opt. **37**, 6164 (1998).

[30] L. Mandel and E. Wolf, *Optical Coherence and Quantum Optics* (Cambridge University, Cambridge, England, 1995).

[31] I. A. Walmsley and C. Dorrer, Characterization of ultrashort electromagnetic pulses, Adv. Opt. Photonics **1**, 308 (2009).

[32] M. Bertolotti, A. Ferrari, and L. Sereda, Coherence properties of nonstationary polychromatic light sources, J. Opt. Soc. Am. B **12**, 341 (1995).

[33] L. Sereda, M. Bertolotti, and A. Ferrari, Coherence properties of nonstationary light wave fields, J. Opt. Soc. Am. A **15**, 695 (1998).

[34] P. Pääkkönen, J. Turunen, P. Vahimaa, A. T. Friberg, and F. Wyrowski, Partially coherent Gaussian pulses, Opt. Commun. **204**, 53 (2002).

[35] H. Lajunen, J. Tervo, and P. Vahimaa, Theory of spatially and spectrally partially coherent pulses, J. Opt. Soc. Am. A **22**, 1536 (2005).

[36] T. Voipio, T. Setälä, and A. T. Friberg, Coherent-mode representation of partially polarized pulsed electromagnetic beams, J. Opt. Soc. Am. A **30**, 2433 (2013).

[37] J. W. Goodman, *Introduction to Fourier Optics*, 3rd ed. (Roberts & Company, Englewood, 2005).

[38] S. A. Collins, Lens-system diffraction integral written in terms of matrix optics, J. Opt. Soc. Am. **60**, 1168 (1970).

[39] H. P. Herzig, Design of refractive and diffractive micro-optics, in *Micro-optics: Systems, Components, and Applications*, edited by H. P. Herzig (Taylor & Francis, London, 1997), Chap. 1, pp. 1–29.

[40] K. Saastamoinen, J. Turunen, P. Vahimaa, and A. T. Friberg, Spectrally partially coherent propagation-invariant fields, Phys. Rev. A **80**, 053804 (2009).

[41] J. Turunen and A. T. Friberg, Propagation-invariant optical fields, in *Progress in Optics*, Vol. 54, edited by E. Wolf (Elsevier, Amsterdam, 2009), pp. 1–88.

[42] J. H. Eberly and K. Wódkiewicz, The time-dependent physical spectrum of light, J. Opt. Soc. Am. **67**, 1252 (1977).

[43] S. A. Ponomarenko, G. P. Agrawal, and E. Wolf, Energy spectrum of a nonstationary ensemble of pulses, Opt. Lett. **29**, 394 (2004).

[44] K. E. Atkinson, *An Introduction to Numerical Analysis*, 2nd ed. (Wiley, New York, 1989).

[45] I. S. Gradshteyn and I. M. Ryshik, *Table of Integrals, Series, and Products*, 7th ed. (Academic, Amsterdam, 2007).